15TH IEA HEAT PUMP CONFERENCE
MAY 26–29, 2026 | HOFBURG
VIENNA 2026
DECARBONISATION THROUGH INNOVATION

A large-scale air heat collector in an air-source heat pump: experiment-based computational analysis of heat transfer duty throughout a frosting cycle with various fin pitches

Valtteri Mikkola[a], Ville Juhola[b], Tero Tynjälä[b]*

[a]*LU-VE Group, Fincoil LU-VE Oy, Ansatie 3, 01740 Vantaa, Finland*
[b] *LUT School of Energy Systems, Lappeenranta–Lahti University of Technology LUT, Yliopistonkatu 34, 53850 Lappeenranta, Finland*

Abstract

Air-source heat pumps play an increasingly central role in low-carbon heating systems. However, their performance under subzero outdoor conditions is significantly constrained by frost accumulation on finned heat exchanger surfaces. Frost build-up not only impedes airflow and increases air-side pressure drop but also degrades thermal conductance, thereby reducing overall system efficiency. Despite its practical importance, experimental data on the relationship between key design parameters, such as fin pitch, and frosting behavior in large-scale heat collectors operating under realistic conditions remain scarce. To address this gap, the present study investigates the influence of two commonly used fin pitches (4 mm and 5 mm) on the thermal performance of air heat collectors. A computational analysis is conducted to evaluate the degradation of heat transfer capacity over time owing to frost formation. The calculation methods for the influence of frost are based on earlier experimental data measured with similar heat exchanger coils in laboratory scale (595 mm x 420 mm x 182 mm). The results indicate that, at 0 °C temperature and 80% or 90% relative humidity, the average heating capacity over a complete operating cycle decreases by 16-26% due to frost accumulation. Consequently, a comparable capacity margin should be incorporated into system design to ensure the desired output. Furthermore, the comparative analysis suggests that a 4 mm fin pitch offers higher heat collection duty than 5 mm throughout the operation cycle, resulting in approximately 5 % higher average duty even under severe frosting conditions. The findings also help identify the optimal timing for defrosting cycles. Overall, this study provides new insights into frost-induced performance degradation and optimal fin design, contributing to more accurate performance prediction and improved design of air heat collectors, particularly relevant to the accelerating electrification of heat production.

Keywords: Air heat pumps; heat collectors; fin pitch; frost; pressure drop;optimization; defrost

1. Introduction

The heat pump market is experiencing rapid growth, driven by environmental concerns and the pursuit of energy self-sufficiency, among other factors [1]. Air-source heat pumps are already a rather common technology for residential heating, and during the last years, industrial-scale heat pump systems have been increasing their share in district heating.

An air heat collector is a component of an air heat pump system, essentially a heat exchanger that transfers heat from ambient air to the working fluid of the heat pump system. Typically, fin-and-tube heat exchangers

* Corresponding author. Tel.: +358445858102
E-mail address: valtteri.mikkola@luvegroup.com

are used for this purpose. As moist air cools down in sub-zero conditions, it imposes the practical challenge of frost forming on the fin side. The frost blocks air passage area, reducing air flow and heat transfer duty [3][4]. In addition, defrosting sequences must be carried out periodically to remove the accumulated frost, which will cause downtime in operation, reducing the effective duty over time [4][5][6].

Predicting and optimizing performance is particularly challenging because air heat collectors operate year-round under highly variable environmental conditions. Therefore, it is essential for the field to be able to consider frosting in a reliable manner in heat collector design and calculations.

Industrial air heat collectors are typically designed with a relatively high fin pitch of at least 4 mm, as wider fin pitch improves endurance under frosting conditions. The wider fin pitch reduces air flow blockage rate and may thus provide a longer operation time [7]. However, increasing fin pitch entails a significant drawback in thermal performance: for example, a fin pitch of 4 mm provides 25% more heat transfer surface area, and thus 5-10% higher duty, than a fin pitch of 5 mm under non-frosting conditions. A significant performance increase can be obtained by optimizing the design parameters [8]. Therefore, a comprehensive analysis based on accurate performance data is required to optimize the design.

This study aims to provide crucial insights into the design and optimization of air heat collector systems. The influence of fin pitch on heat transfer duty throughout a complete frosting cycle is studied computationally. A step-based calculation algorithm is developed to evaluate how the thermal duty of heat collectors with fin pitches of 4 mm and 5 mm decrease over time due to frost accumulation. All correlations and methods used for frost performance calculations are based on comprehensive experimental studies previously conducted by the research group using comparable test coils in laboratory conditions [9].

The calculations are performed for typical heat collector design conditions, with ambient air temperature of 0 °C and relative humidities of 80% and 90%. The results reveal which fin pitch yields higher total heat collection over an entire operating cycle. Furthermore, the study quantifies the additional design margin required to compensate for frost-induced performance degradation and provides guidance on optimal defrosting intervals for air heat collectors.

2. Methods

The heat transfer duties of heat collectors with fin pitches of 4 mm and 5 mm were computationally determined over a complete frost cycle in this study. The heat collector configurations analyzed correspond to the real LU-VE Solar SHD 7B 09TE N5 6D IF4/5 CU198 model, which is typically used in industrial-scale applications [10]. Likewise, the temperature and fluid flow conditions represent a typical design point of a heat collector operating under frosting conditions. Freezium 40% (potassium formate HCOOK, water, corrosion inhibitors) is used as a working fluid. The configurations of the heat collectors and the operating conditions are presented in Table 1.

Table 1 Heat collector configuration and operation conditions

Fluid name	Freezium 40%	Freezium 40%	Freezium 40%	Freezium 40%
Fluid flow (kg/s)	38.0	38.0	38.0	38.0
Temperature in (°C)	-8.0	-8.0	-8.0	-8.0
Air temperature in (°C)	0	0	0	0
Air humidity (%)	80	90	80	90
Heat transfer area (m²)	2473	2474	2022	2022
Tube diameter (mm)	12.7	12.7	12.7	12.7
Coil length (mm)	12600	12600	12600	12600
Coil width (mm)	2310	2310	2310	2310
Coil depth (mm)	182	182	182	182
Number of tubes per row	66	66	66	66
Number of tube rows	6	6	6	6
Fin type	Wavy	Wavy	Wavy	Wavy
Fin spacing (mm)	4	4	5	5
Fin thickness (mm)	0.25	0.25	0.25	0.25
Fan	Ziehl ZN100	Ziehl ZN100	Ziehl ZN100	Ziehl ZN100
Fan type code	ZIL.GL.V5P1	ZIL.GL.V5P1	ZIL.GL.V5P1	ZIL.GL.V5P1
Fan pcs	14	14	14	14
Fan rpm	500	500	500	500

The calculation was carried out point by point with a time interval of 20-37 s, starting from the initial time t0=0s, when the coil had no frost but exhibited a positive frosting rate. The amount of frost at each subsequent time step was determined based on the frosting rate calculated at the previous step. As frost accumulates, the pressure drop across the coil increases, leading to a reduction in air flow. The heat duty and the new frosting rate were then recalculated based on the updated air flow. All performance parameters were computed iteratively in Microsoft Excel until a predefined maximum simulation time was reached.

2.1. Assumptions based on experimental background

Computational modeling in this study is based on experiments conducted using identical heat collector coils tested at laboratory-scale under controlled laboratory conditions. The test setup is presented in Figure 1. The earlier results are clarified in [9].

The key experimentally verified input parameters and assumptions used in the modeling are as follows:

- The humidity loss rate on the air side corresponds directly to the frosting rate (frost mass accumulating on the coil as kg/s).
  - Water / frost do not exit the system during operation.
- The frost layer thickness is assumed to be uniform across the entire heat transfer surface.
  - Experiments indicated uniform frost distribution in the conditions studied close to 0 °C ambient temperature. However, further tests in other conditions indicated that in sub-zero temperatures frost layer thickness may not be as uniform.
- The frost density under these conditions is 150 kg/m³.
- The thermal conductance remains approximately constant at a constant air flow.
- The pressure drop across the frosted coil follows the Equation 2 presented below.

Figure 1 The laboratory-scale test setup with coil size of 595 mm x 420 mm x 182 mm [9]

2.2. Pressure loss equation for frosted coil

Previous experiments conducted by the research group [9] concluded that the influence of frost on the air-side pressure drop, under conditions of constant air flow, can be modeled as a function of the reduction in the minimum cross-sectional flow area as:

$$\Delta p_{\mathrm{ref},n} = \Delta p_0 \cdot \left(\frac{A_{\mathrm{cross},n}}{A_{\mathrm{cross},0}}\right)^{3.7} \tag{1}$$

where $\Delta p_{\mathrm{ref},n}$ is the reference pressure drop across the coil assuming the initial air flow, Δp_0 is the initial pressure loss for a clean (non-frosted) coil, $A_{\mathrm{cross},n}$ is the minimum cross-sectional flow area in a single gap constrained by frosted fins and tubes, and $A_{\mathrm{cross},0}$ is the initial minimum cross-sectional flow area in a single gap constrained by clean (non-frosted) fins and tubes.

The experimental data for the 5 mm coil is presented in [9]. In addition, the 4 mm coil was tested and the applicability of the frost pressure drop equations for 4 mm was thus also confirmed experimentally, as presented in Figure 2.

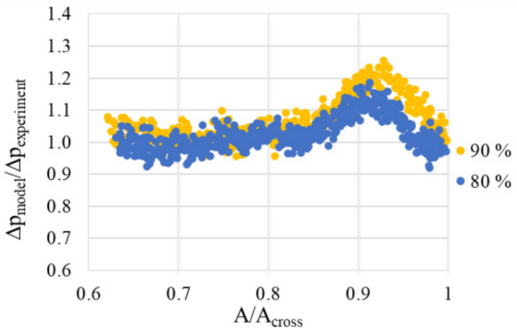

Figure 2 The model vs experimental pressure drop data for 4 mm coil with 80% and 90% humidity.

Generally, the pressure drop in a fixed system is roughly directly proportional to the square of the flow rate. When considering also varying air flow rate, the pressure drop can be calculated as

$$\Delta p_n = \Delta p_{\mathrm{ref},n} \cdot \left(\frac{\dot{V}_n}{\dot{V}_0}\right)^2 = \Delta p_0 \cdot \left(\frac{A_{\mathrm{cross},n}}{A_{\mathrm{cross,0}}}\right)^{3.7} \left(\frac{\dot{V}_n}{\dot{V}_0}\right)^2 \tag{2}$$

where $\dot{V}_n$ is the air flow rate.

2.3. Air flow

Air flow of a heat collector is driven by several fans that are typically mounted on top of the unit. The heat collector studied herein has 14 pieces of Ziehl ZN100 ZIL.GL.V5P1 fans. In this study we model their performance based on manufacturer's datasheet curve [11]. The fans operate at rotation speed of 500 rpm, which represents a typical rotation speed for heat collection applications. The fan curve is corrected to air density of this study, 1,292 kg/m^3 in 0 °C air. The fan curve at 500 rpm is presented in Figure 3.

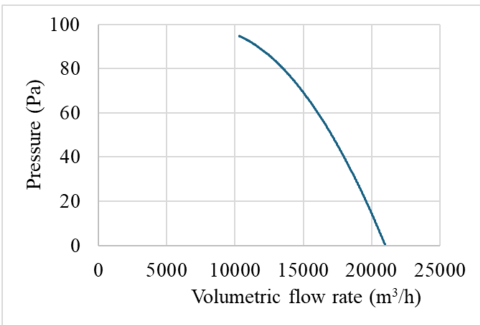

Figure 3 Fan performance curve

Frost formation causes the coil pressure drop to increase, and therefore, the air flow rate decreases in real heat collector applications where the fans operate at constant rotational speed. This may cause fan performance to drop to its stalling point. In the stalling point, fan performance deteriorates sharply, resulting in a significant reduction in air flow, efficiency, and acoustic performance. Also fan manufacturers typically recommend not operating fans in the stalling area [11]. Therefore, in real applications, the defrost sequence should be initiated before the system reaches the stalling point to restore the designed performance. This is what we assume also in this study: defrosting is initiated at the latest when fan approaches near its stalling point and air flow per fan decreases to minimum value of 10300 m^3/h. In this study, the calculation length for each case is determined so that fan reaches minimum air flow value (stalling point) at the last calculated time point.

The pressure increase of the fan is equal to the coil pressure drop, since the air both before and after the unit is in same ambient pressure (other pressure drops are considered negligible). The pressure difference produced by the fan Δp_{n} in the appropriate operation region above the stalling point can be presented with good accuracy by using a second order polynomial

$$\Delta p_n = 0.0000005714 * \dot{V}_n^{\,2} + 0.0090299141 * \dot{V}_n^{\,2} + 62.3634 \quad (3)$$

Finally, the pressure drop Δp_n and volumetric flow rate $\dot{V}_n$ can be solved based on the Equations 2 and 3, when remaining cross-sectional flow area $A_{\text{cross},n}$.is calculated

2.4. Amount of frost and remaining cross-sectional flow area

The minimum cross-sectional flow area in a single gap $A_{\text{cross},n}$ under frosted conditions is the key parameter for calculating the pressure drop of the frosted coil. To calculate $A_{\text{cross},n}$, the frost thickness on all heat transfer surfaces is required. In this study, we assume that the frost is distributed uniformly across all heat transfer surfaces. This was shown to be a reasonable approach under the studied conditions by [9]. Under different temperature and humidity conditions, however, the coil surface temperature may fall below the dew point only in certain regions; in such cases, the assumption of uniform frost distribution would no longer be valid. For example, other similar experiments of the group have indicated that the frost accumulation on outlet side may get emphasized already in slightly lower temperatures, and behavior close to 0 °C is highly sensitive on temperature.

The frost thickness l_n is calculated from the frost mass $m_{\text{frost},n}$, frost density ρ and total heat transfer surface area A_{tot} as:

$$\mathrm{l_n} = \frac{m_{\text{frost},n}}{\rho A_{\text{tot}}} \quad (4)$$

In this study, ρ is assumed to be 150 kg/m^3. In earlier experiments this density was noticed to apply with good accuracy in these conditions based on comparing measured frost weight to frost thickness determined based on camera images [9]. This density also results in a good correspondence between the measured pressure loss and pressure loss predicted based on Eq 2. In general, frost density is strongly dependent on temperature conditions, and therefore this experiment-based density assumption is only valid close to the studied conditions. In case of other temperatures, density could be evaluated based on established correlations, although this would cause significant uncertainty since frost density is highly sensitive on conditions [12][13].

The frost mass is initialized at zero, and its value at any subsequent time step n is calculated simply based on the cumulative frost mass and the frosting rate $\dot{m}_{\text{frost},n-1}$ at the previous step $n-1$, as:

$$m_{\text{frost},n} = m_{\text{frost},n-1} + \dot{m}_{\text{frost},n-1}\Delta t \quad (5)$$

In this study, each calculation case contained 200 time steps, resulting in time step length Δt of 20-37 s.

When the frost thickness is known, the minimum cross-sectional area in a single gap constrained by frosted fin and tube can be calculated as

$$A_{\text{cross},n} = \left(F_{\text{p}} - \lambda - 2\mathrm{l}_n\right) * (P_t - D_o - 2\mathrm{l}_n) \quad (6)$$

where F_{p} is the fin pitch, λ is fin thickness, P_t is the tube pitch and D_o is the tube outer diameter

2.5. Heat transfer duty and frosting rate

Generally, the heat transfer duty of a heat exchanger depends on several factors, such as logarithmic mean temperature difference, flow rates, fluid properties, phase change phenomena on the fin side, geometrical characteristics of the heat exchanger, fouling or other resistance such as frost, fin efficiency, and many others. In this study, we utilize heat collector coil manufacturer's (LU-VE group) calculation program to construct a performance curve as a function of air flow rate. Since frosting affects the air flow rate, the corresponding heat transfer duty was determined based on this curve. The program was also utilized to generate the frosting rate curve as a function of air flow. Both the duty and frosting rate curves are presented in Figure 4.

The thermal resistance of frost was considered by fine-tuning the program's calculations with extra thermal resistance based on the finding of [9], that the thermal conductance under frosted conditions is approximately equal to that of a clean coil when the air flow is equal. Physically, this implies that the added thermal resistance of the frost layer roughly corresponds to the increase in the air-side heat transfer coefficient caused by higher velocities in the narrowed, frost-covered flow passages. In this study, however, the fan performance is also considered, and therefore the air flow rate does not remain constant but decreases as frosting progresses, leading to a corresponding reduction in the overall thermal conductance.

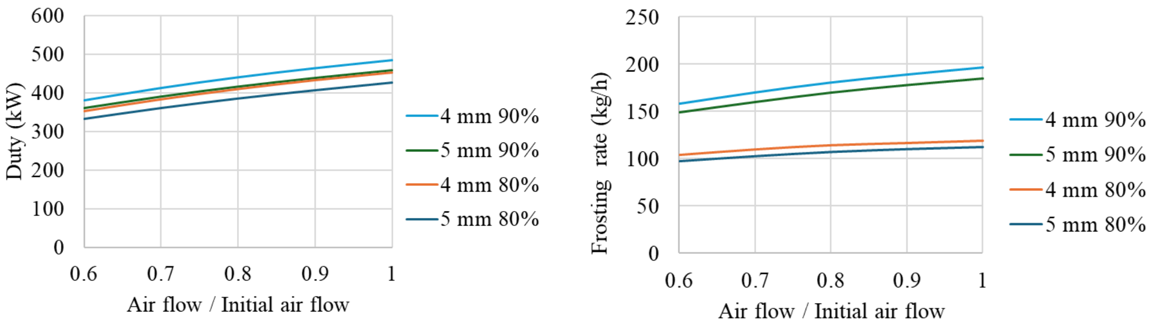

Figure 4 Duty and frosting rate curves

2.6. Key result parameters in a cycle

A real industrial heat collector system typically consists of several, or even dozens of, individual units. These units operate at different stages of the frost-defrost cycle: some operate at full performance under clean conditions, some are slightly or heavily frosted, and others are temporarily out of operation owing to defrosting. Therefore, the overall duty of the entire system corresponds to the average duty over a complete frosting cycle, considering also the downtime associated with defrosting.

To evaluate the overall performance of the heat collector system, it is necessary to analyze the average heat collection duty throughout the cycle. At each time step, the cumulative collected heat $E_{\mathrm{cum},n}$ is determined as the sum of the heat collected in all previous steps. The average duty is then obtained by dividing the cumulative heat by the total cycle time. However, it is important to include also defrosting period in this analysis to obtain a comprehensive picture of system performance and to be able to analyze the optimal timing for defrost initiation. At any given point, if defrosting was initiated, the total cycle time would be the sum of the operating time and the defrost duration. Therefore, the average duty $P_{\mathrm{ave},n}$ including also defrost downtime is expressed as:

$$P_{\mathrm{ave},n} = \frac{E_{\mathrm{cum},n}}{t_n + t_{\mathrm{defrost}}} \tag{7}$$

where t_{defrost} is the downtime due to defrost. In this study, we consider the downtime to be 10 minutes, which corresponds to a typical defrosting time in real large-scale applications. In addition, we determine the average net duty $P_{\mathrm{net,ave},n}$ to provide also indication of magnitude of the energy loss required for defrosting. However, the average net duty should be considered only as an indicative measure for defrost energy loss, because the energy collected and energy used for defrosting are at different temperature levels, and thus netting them in such a direct manner is not entirely physically meaningful.

$$P_{\mathrm{net,ave},n} = \frac{E_{\mathrm{cum},n} - \frac{m_{\mathrm{frost},n} * l_{\mathrm{melt}}}{EFF_{\mathrm{defrost}}}}{t_n + t_{\mathrm{defrost}}} \tag{8}$$

where l_{melt} is melting heat of frost 334 kJ/kg and EFF_{defrost} is the defrost efficiency, which we assume to be 50%. The defrosting time 10 min and efficiency 50 % are of obviously rough estimates and in reality, they vary between applications. However, these parameters have only a limited impact on the final conclusions of the study, so it is better to consider them even with rough estimates.

3. Results and discussion

The performance of air heat collectors with fin pitches of 4 mm and 5 mm was computationally analyzed in this study to determine the optimal fin pitch, the duty loss due to frost, and the optimal defrosting time. The analysis was carried out under typical operating conditions, with an ambient temperature of 0 °C and relative humidities of 80% and 90%.

Heat collection duty and frost thickness calculated throughout the operating cycle are presented in Figure 5. As expected, the heat collection duty decreases as the frost thickness increases. At the end of the cycle, the frosted duty values are approximately 20% lower than the clean duty at the beginning, confirming that frost formation has a significant impact on system performance and must be considered in the design of heat collector systems. The 4 mm fin pitch exhibits higher performance than the 5 mm throughout the operating cycle. Although the performance of the 4 mm coil decreases slightly more steeply due to frost accumulation, it still maintains a higher performance even at the end of the cycle, indicating higher overall performance. The 4 mm fin pitch has a slightly shorter maximum operating cycle duration (11-13%) than the 5 mm coil, as expected. The frost thickness grows slightly slower for the 4 mm fin pitch, simply because the frost is distributed over a larger heat transfer surface area.

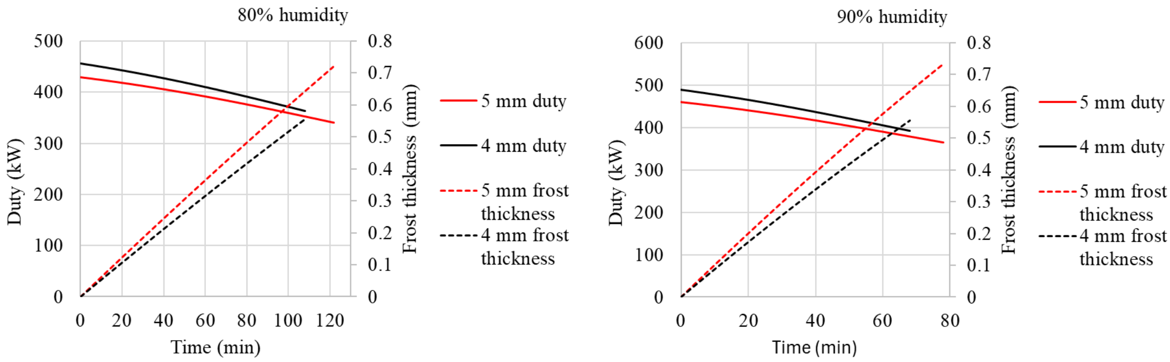

Figure 5 Heat collection duty and frost thickness as a function of operation time.

Figure 6 presents the average duty and average net duty depending on the operation cycle length. Each point represents the average duty that would be achieved if operation was stopped and defrosting initiated at that specific moment. The curves start from zero, representing that too frequent defrosting is not optimal for heat collection due to defrost downtime. The highest point represents the optimal time to stop operation and start defrosting: this operation time yields the maximum average duty or net duty considering the entire cycle. The optimum point in all curves is close to the longest calculated operation, where the fan reaches stalling point. However, the curves are almost horizontal at the end of the cycle, indicating that a perfect optimization of cycle length has only a negligible influence. As a general rule with this configuration, the operation should be continued for as long as possible and defrost initiated just before fan stalling point would cause a rapid decrease in performance.

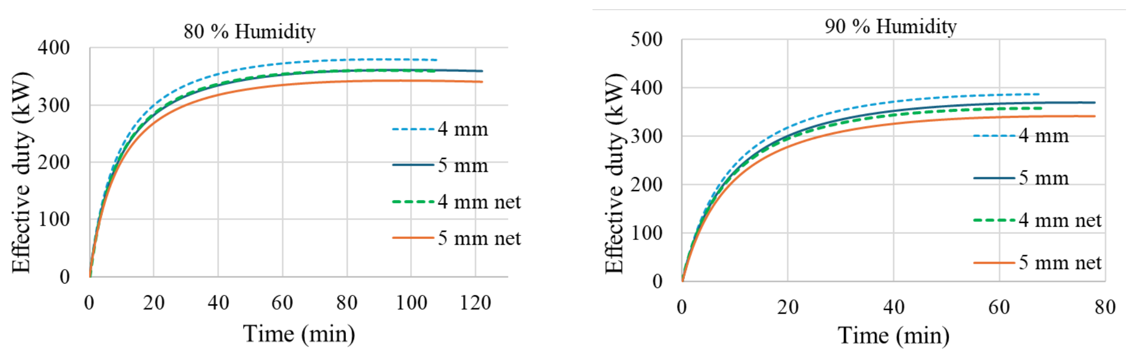

Figure 6 Average heat collection duty and net duty over time.

These results pronounce the importance of fan design in heat collectors, since the optimal operation length can be to continue operation close to the fan stalling point, particularly in case of high humidity. Enough margin must be reserved between the design clean point and stalling point to ensure appropriate frost endurance. Several fans available would stall even faster resulting in shorter operation cycle and reduced average duty over a complete cycle. Additionally, the fan curve should preferably keep air flow as high as possible despite the increasing pressure drop. For many fan types, also sound may increase notably when pressure increases, which should be avoided, since many heat collector fields are designed to operate within the maximum allowable sound limit. However, the aspect of sound was outside the scope of this study.

The maximum average duties and net duties are presented in Table 2 along with initial clean design duties. In case of 80% humidity, the maximum average duties and net duties are approximately 16% and 20% lower than the clean design duty. In case of 90% humidity, the difference becomes even higher, as expected: 20% and 26%. This means that a corresponding design margin should be reserved when designing a new system under frosting conditions, if the design duty calculation is based on the clean duty. Average net duties are 4-6 %-units lower than average duties, indicating that a defrost energy loss is significant and should be considered in real system design. The maximum average net duties are almost equal with both humidities, indicating that a higher humidity does not yield higher performance under frosting conditions, when the complete operating cycle is considered. All average duties are lower than the clean duties calculated with dry air, 376 kW for 5 mm and 400 kW for 4 mm coils. The seemingly beneficial increment in the clean duty owing to humidity is outweighed by frost penalty and defrosting consumption, which is in line with lower COP values often reported due to high humidity under frosting conditions [14]. Therefore, a high design humidity in heat collector system dimensioning should be avoided, as it can result in an unrealistically high impression of performance. In addition, efficient modern defrosting strategies and optimal operation cycle lengths, such as reported in this study, should be employed to mitigate the performance loss caused by frost.

Table 2 maximum heat collection duties, net duties, optimum operation cycle lengths and clean duties.

Fin pitch (mm)	Air humidity (%)	Clean duty (kW)	Max ave duty (kW)	Opt operation time (min)	Max ave net duty (kW)	Opt operation time net (min)	Stalling time (min)
4	80	453	380	92	360	91	108
5	80	427	362	98	343	96	122
4	90	485	387	68	358	68	68
5	90	458	370	75	342	74	78

Based on the results, the 4 mm fin pitch outperforms the 5 mm even under frosted conditions, achieving approximately 5% higher maximum net duty. In addition, the 4 mm fin pitch would also provide higher performance throughout the year during non-frosting conditions. Therefore, a 4 mm fin pitch should be preferred over 5 mm in practical application design. The additional material cost associated with the smaller fin pitch is typically minor, meaning that the investment cost per kilowatt of heat duty would also improve when using a 4 mm fin pitch instead of 5 mm.

An obvious next question is whether an even lower fin pitch would perform better yet. However, extending the present analysis to lower fin pitches would be highly speculative, since the experimental data underlying this study were available only for the 4 mm and 5 mm configurations. Additional experiments with lower fin pitches would be required to establish reliable conclusions. Based on earlier studies, influence of frost is expected to be even more pronounced with yet smaller fin pitches, as fin pitch is reported to be a crucial parameter controlling the frosting dynamics [15][16]. Therefore, we conclude by proposing 4 mm as a preferable fin pitch for industrial-scale air heat collectors, when a comparable coil configuration is used. The phenomena studied herein are dependent on many coil parameters, and therefore firm conclusions for other coil configurations cannot be drawn. However, we hypothesize the benefit of 4 mm fin pitch to hold also for looser coil geometries (i.e. larger tube pitches), since they typically benefit from the higher heat transfer surface area even more, while the drawback due to higher pressure drop is lower. On the contrary, for tighter tube configurations the same conclusions may not hold, but such compact geometries are unlikely to be favorable for industrial heat collectors in any case, due to their lower expected frost endurance.

Similar step-based computational algorithms could be employed to design programs to estimate heat collector duty over an entire frosting cycle. This would increase the predictability of system performance and allow better design optimization, resulting in lower investment risks and increased efficiency. However, the calculation is dependent on pressure drop equations and frost densities used in the calculation, which should be experimentally verified for the studied configurations and conditions, such as was done for this study.

4. Conclusions

The influence of frost on air heat collector duty was computationally studied. The performance of a typical heat collector configuration with fin pitches of 4 mm and 5 mm was calculated over a complete frosting cycle under typical operating conditions. The calculation model was based on earlier extensive laboratory measurements carried out with the similar heat collector coils under the same conditions.

Frost was observed to have a significant influence on the heat collection performance. The average duty over the entire cycle was 16-20% lower than the clean design duty and the net duty considering also energy lost for defrosting was 20-26% lower. A corresponding design margin must be reserved when designing a new heat collector system.

The 4 mm fin pitch was observed to provide higher heat collection duty even in challenging frosting conditions. Despite a slightly shorter operation cycle, the 4 mm configuration had higher performance throughout the cycle resulting in 5% higher average duty. Based on these results we propose 4 mm as a preferable fin pitch for industrial heat collector design, when a comparable coil configuration is used.

With the studied configurations, the optimal defrost time was close to fan stalling point, indicating that the operation should be continued for as long as possible without stalling before initiating defrost. However, the average duty curve is almost constant close to the optimum point, meaning that defrosting slightly earlier would have only a minor impact on the average duty.

Acknowledgements

Authors acknowledge the support by Business Finland under the project 'NEXTHEPS - Development of Next Generation Large Scale Heat. Pump Systems (grant number: 1535/31/2022)'.

References

[1] Eurostat, Renewable energy for heating & cooling up to 25% in 2022, (2024). https://ec.europa.eu/eurostat/web/products-eurostat-news/w/ddn-20240227-2
[2] F. Gerard, T. Smit, K. Rademaekers, S. Braungardt, M. Monejar Montagud, L. Guevara Opinska, Policy support for heating and cooling decarbonisation : roadmap, Publications Office of the European Union, 2022. Doi: doi/10.2833/ 977806.
[3] D.L. Da Silva, C.J.L. Hermes, C. Melo, Experimental study of frost accumulation on fan-supplied tube-fin evaporators, Appl Therm Eng 31 (2011) 1013–1020. https://doi.org/10.1016/j.applthermaleng.2010.11.006.
[4] C.T. Sanders, Frost Formation The Influence of Frost Formation and Defrosting on the Performance of Air Coolers, 1974.
[5] P.L.T. Brian, R.C. Reid, Y.T. Shah, Frost Deposition on Cold Surfaces, Industrial & Engineering Chemistry Fundamentals 9 (1970) 375–380. https://doi.org/10.1021/i160035a013.
[6] W. Wang, Y.C. Feng, J.H. Zhu, L.T. Li, Q.C. Guo, W.P. Lu, Performances of air source heat pump system for a kind of mal-defrost phenomenon appearing in moderate climate conditions, Appl Energy 112 (2013) 1138–1145. https://doi.org/10.1016/j.apenergy.2012.12.054
[7] Lee, W.-J., Bae, K. J., & Kwon, O. K., Effect of hydrophobic surfaces on frost retardation in fin-tube heat exchangers with various fin pitches. Applied Thermal Engineering 176 (2020), 115424. https://doi.org/10.1016/j.applthermaleng.2020.115424
[8] Yang, D.-K., Lee, K.-S., & Song, S. Fin spacing optimization of a fin-tube heat exchanger under frosting conditions. International Journal of Heat and Mass Transfer, 49(15), 2006, 2619–2625. https://doi.org/10.1016/j.ijheatmasstransfer.2006.01.016
[9] Juhola et. Al. A wavy fin-and-tube heat exchanger in an air-source heat pump: Experimental results on the influence of frost on air-side pressure drop and thermal performance. Applied Thermal Engineering 287 (2025), 127396
[10] LU-VE Group website, Solar Series, https://alfa.luvegroup.com/ssr
[11] Ziehl-Abegg, Performance Data, https://www.ziehl-abegg.com/en-fi/detail/FE2owlet%20mit%20ZAplus/ZN100-ZIL.GL.V5P1/184683
[12] Y. Hayashi, A. Aoki, S. Adachi, K. Hori, Study of frost properties correlating with frost formation types, J. Heat Transfer 99, 1977, 239–245. https://doi.org/ 10.1115/1.3450675

[13] C.J.L. Hermes, F.R. Loyola, V.S. Nascimento, A semi-empirical correlation for the frost density, Int. J. Refrig 46 ,2014 100–104. https://doi.org/10.1016/j. ijrefrig.2014.02.008
[14] P. Vocale, G.L. Morini., M. Spiga, Influence of outdoor air conditions on the air source heat pumps performance, 68th conference on the italian thermal machines engineering association ATI2013, Energy procedia (2014) 653-662.
[15] Zhang, L., Jiang, Y., Dong, J., Yao, Y., & Deng, S., An experimental study on the effects of frosting conditions on frost distribution and growth on finned tube heat exchangers. International Journal of Heat and Mass Transfer 128, 2019, 748-761. https://doi.org/10.1016/j.ijheatmasstransfer.2018.09.016
[16] Ji, J., Zhao, J., Ni, X., Pan, Y., & Li, Y., An experimental study on the influence of base plate temperature and fin pitch on frosting characteristics of parallel cold plates. Case Studies in Thermal Engineering, 71, 2025, 106209. https://doi.org/10.1016/j.csite.2025.106209